Int. J. Engng Sci., 1974, Vol. 12, pp. 221–243. Pergamon Press. Printed in Great Britain

THREE-DIMENSIONAL HARMONIC FUNCTIONS NEAR TERMINATION OR INTERSECTION OF GRADIENT SINGULARITY LINES: A GENERAL NUMERICAL METHOD

ZDENĚK P. BAŽANT†
Department of Civil Engineering, Northwestern University, Evanston, Illinois 60201, U.S.A.

Abstract—The harmonic function u near point 0 from which a single singularity ray emanates is assumed to be dominated by the term $r^{\lambda}\rho^{p}U$ where r=distance from point 0, p=known constant and ρ=chosen function of angular spherical coordinates θ, φ, for which a partial differential equation with boundary conditions, especially those at the singularity rays, and a variational principle, are derived. Because grad U is nonsingular, a numerical solution is possible, using, e.g. the finite difference or finite element methods. This reduces the problem to finding λ of the smallest real part satisfying the equation Det $(A_{ij})=0$ where A_{ij} is a large matrix whose coefficients depend linearly on $\mu=\lambda(\lambda+1)$. In general λ and A_{ij} are complex. Solutions can be obtained either by reduction to a standard matrix eigenvalue problem for μ, or by successive conversions to nonhomogeneous linear equation systems. Computer studies have confirmed the feasibility of the method and have shown that highly accurate results can be obtained. Solutions for cracks and notches ending at a plane or conical surface, and for cracks ending obliquely at a halfspace surface, are presented. In these cases, λ is real and the singularity is always weaker ($\lambda>p$) than on the singularity line and may even disappear ($\lambda>1$). Furthermore, elastic stresses under a wedge-shaped rigid sliding stamp or at a corner of a crack edge, and also harmonic functions at three-sided pyramidal notches, have been analyzed. Here $\lambda<p$ was found to occur. A simple analytical solution for one class of special cases has also been found and used to check some of the numerical results.

INTRODUCTION

IN THREE-dimensional potential theory there exists a great number of problems in which one or several lines of singularity of the potential gradient terminate or intersect. The singularity at the point of termination or intersection can naturally be expected to differ from the singularity on the line or lines entering this point. Solutions to these problems are of considerable interest, e.g. for scattering of waves at a corner of a screen, for distribution of electric charge, for problems of heat conduction, potential flow, seepage etc., and perhaps most importantly, for fracture mechanics of elastic bodies. At present, however, most of these problems remain unsolved.

One problem of this type is the distribution of pressure below the tip of a rigid frictionless stamp of wedge-shaped contact, pressed upon an elastic halfspace. The problem can be reduced to a potential theory problem[4]. It was discussed in 1947 by Galin[5, 4] and an approximate solution restricted to non-oscillating singularities and based on mapping of a hemisphere upon a circle was presented in 1957 by Rvachev[11]. He applied the Galerkin method in the mapped domain and, using up to six terms, made rough estimates of the real values of the singularity exponent λ. He concluded that the pressure near the tip behaves as $r^{\lambda-1}$ where λ monotonously increases from 0 to 1 as the wedge angle 2α grows from 0 to 2π (r = distance from the tip). Recently Aleksandrov and Babeshko[1] used Green's function approach to study analytically the limiting case of the wedge angle 2α tending to zero. They concluded that near the tip the pressure exhibits an oscillating singularity of the type $r^{-1\cdot5}\cos(k\ln r)$ (k = parameter), which obviously prevails over the non-oscillating singularity r^{-1} found for $\alpha\to0$ by Rvachev[11].

†Professor of Civil Engineering.

But it seems that no complete solutions of the near singularity fields, including the singularity on the edge of the stamp near the tip, have been presented so far.

A mathematically equivalent problem for the Helmholtz reduced wave equation, consisting in wave scattering near the tip of a right-angled corner of a screen, was studied analytically by Radlow [9]. He found that near the tip the harmonic wave function is of the type $r^{0.25}$, without checking for a possible imaginary part of the exponent, and without deducing the near-tip field itself. Diffraction of elastic waves by a right-angled wedge was also studied analytically by Kraut [16].

The intent of the present study is to propose a general method for problems of this type. The method will consist of reduction to a two-dimensional eigenvalue problem for a function without gradient singularity, which can presumably be solved numerically with any desired accuracy.

TYPE OF PROBLEMS TO BE DISCUSSED

Using spherical coordinates θ, ϕ, r, the Laplace equation for the potential $u(\theta, \phi, r)$ reads

$$\nabla^2 u = \frac{\partial^2 u}{\partial r^2} + \frac{1}{r^2}\frac{\partial^2 u}{\partial \theta^2} + \frac{1}{r^2 \sin^2\theta}\frac{\partial^2 u}{\partial \phi^2} + \frac{2}{r}\frac{\partial u}{\partial r} + \frac{\cot\theta}{r^2}\frac{\partial u}{\partial \theta} = 0. \tag{1}$$

The problem to be discussed herein consists in finding the limiting form of the solution of this equation as $r \to 0$, assuming that the domain of the solution is an infinite space bounded by a certain surface $B(\theta, \phi) = 0$ formed by rays emanating from point 0. The boundary conditions are $u = 0$ on part of the surface and $\partial u/\partial n = 0$ on the remaining part, n being a normal to the surface. (The case of the boundary conditions $u =$ constant on part of the surface is easily reduced to the present case.) No boundary conditions will be prescribed at any point on radial rays that do not lie entirely on $B = 0$, so that an infinite number of solutions can be expected. Assuming these solutions to comprise a complete system of linearly independent functions, a certain linear combination of these solutions should satisfy the additional boundary conditions on the radial rays occurring in real problems. As will be seen, a class of admissible solutions is of the form $r^\lambda F(\theta, \varphi)$ and consequently, regardless of the type of the afore-mentioned linear combination, the solution for any boundary conditions on the radial rays will be dominated in a sufficiently small neighborhood of point 0 by that solution of the present problem for which $Re(\lambda)$ is *smallest*. When $Re(\lambda) < 1$, grad u near point 0 becomes unbounded, i.e. the solution exhibits a singularity at point 0. However, for the given boundary conditions on the radial rays the singularity need not necessarily occur because the solutions with $Re(\lambda) < 1$ need not be present in the afore-mentioned linear combination (as in the case of a homogeneous normal stress field parallel to a crack). The sufficient conditions of singular behavior, as well as the uniqueness aspects, cannot be included in the present study.

If u is required to be finite, only $Re(\lambda) > 0$ is admissible. (However, in some physically meaningful problems, such as the case of a line load on an elastic half-space, u is not finite at point 0.)

The surface formed by radial rays and the corresponding boundary conditions are assumed to be of such a form that the surface contains a finite number of rays on which grad u is singular (unbounded). Further, it is assumed that at any finite distance L from point 0, the field within a neighborhood of the singularity ray which is sufficiently smal-

ler than L is known, and is of the same type at any point of the ray except at point 0. This field may be determined by solving the plane problem in a plane normal to the ray. (The latter property is verified in some special cases by the analytical solutions reported in the sequel.)

Consider the plane section normal to a singularity ray passing through point 0′ at a finite distance L from point 0. It is assumed that within a neighborhood of point 0′ which is sufficiently smaller than L, the normal plane section of the body is bounded by two straight rays $0'A$, $0'B$ from point 0′, forming angle α (Fig. 1). The boundary condition on the rays may be either $u=0$ or $\partial u/\partial\phi=0$ where ϕ = angular coordinate in Fig. 1. The solution near point 0′ in the normal plane section may be sought in the form $u \sim r_1^p f_1(\phi)$ where r_1 is the distance from point 0′, and p and $f_1(\phi)$ are assumed to be the same at any finite distance L from point 0.

To give an example of the determination of p and $f_1(\phi)$, consider that the boundary conditions are $\partial u/\partial\phi=0$ on ray $0'A$, and $u=0$ on ray $0'B$. Substitution of $u=r_1^p f_1(\phi)$ into the Laplace equation yields a homogeneous ordinary differential equation for $f_1(\phi)$, whose general solution is $A\cos p\phi + B\sin p\phi$. The boundary conditions reduce to $df_1(0)/d\phi = 0$, $f_1(\pi-\alpha)=0$, which yield

$$u \sim r^p f_1(\phi) \quad \text{where} \quad f_1(\phi)=\cos p\phi,\ p=\tfrac{1}{2}\pi/(\pi-\alpha). \tag{2}$$

The same result is obtained when rays $0'A$, $0'B$ form angle 2α and $u=0$ on both rays.

This technique of the determination of the near-singularity fields has been used in plane elasticity (where it is not as trivial as here) by Knein[8] (who thanked T. von Kármán for suggesting the basic approach), and later independently by Williams[14] and Karp and Karal[7]. In analogy with this technique, the variables may be separated in the three-dimensional problem as follows:

$$u(\theta, \phi, r) = r^n f(\theta, \phi) \tag{3}$$

where n is, in general, complex and f is a function of θ and ϕ only. It may be imagined as a function defined in a certain domain Ω on a unit sphere about point 0. Substitution of (3) into the Laplace equation (1) allows r to be completely eliminated from the equation and results in a differential equation for $f(\theta, \phi)$.

It should be noted that in the case of the Helmholtz reduced wave equation, $\nabla^2 u + k^2 u = 0$ (arising in wave scattering problems), or the Poisson equation, $\nabla^2 u = k$, the variable r is not eliminated since the additional term $k^2 r^2 f$ or kr^{2-n}, respectively, appears in the equation for f. However, in a sufficiently small neighborhood of point 0, this term becomes negligible, as compared with other terms in the equation (provided that f is

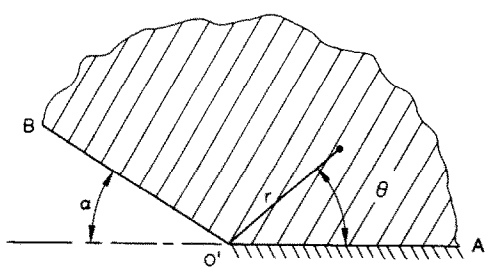

Fig. 1. Planar case giving rise to singularity at point 0′.

bounded and, in the case of the Poisson equation, $n<2$). Thus, the solutions of the reduced wave equation and the Poisson equation exhibit the same type of singularity as the harmonic functions.

The gradient singularity at point 0 is only partly interpreted by the term r^n in equation (3) since along certain radial rays there is an additional singularity which must be embedded in function f. Consequently, function f is not suitable for determination by approximate numerical methods.

REMOVING SINGULARITY ON RADIAL SURFACE RAYS

It is desired to separate the variables in such a manner that, in any plane normal to the singularity ray, function u near the ray be of the same form as equation (3) in which f_1 has no gradient singularity. Considering, for the sake of brevity, the case of a single singularity ray, this may be achieved by writing

$$u(\theta, \phi, r) = r^n r_1^p U(\theta, \phi) \tag{4}$$

where r_1 = chosen continuous smooth function of θ, ϕ, and r, which is identical to the distance from the singularity ray in its vicinity and is nonzero everywhere except on the ray. Obviously, if p is the correct exponent for the gradient singularity on the ray, as determined from (2), $U(\theta, \phi)$ must be a continuous smooth function of θ and ϕ which has (a) no gradient singularity on the singularity ray, and (b) in its vicinity is proportional to the function f_1 from equation (2).

Function r_1 may always be introduced in the form

$$r_1 = r\rho(\theta, \phi) \tag{5}$$

where ρ = chosen continuous smooth function of θ and ϕ which is nonzero everywhere except on the singularity ray in whose vicinity it is identical with the distance from the ray measured on the unit sphere. Thus

$$u(\theta, \phi, r) = r^\lambda F(\theta, \phi) = r^\lambda \rho^p U(\theta, \phi) \tag{6}$$

where

$$\lambda = n + p. \tag{7}$$

If the singularity ray is located at the pole, $\theta = 0$, a very simple choice of ρ is possible:

$$\rho = \theta \quad \text{or} \quad \rho = \sin\theta. \tag{8}$$

With the latter choice, r_1 represents the exact distance from the ray not only in its vicinity but everywhere in the domain. It must be warned, however, that $\sin\theta$ cannot be used when $\theta = \pi$ is part of the domain and no singularity ray exists at $\theta = \pi$. The function $\rho = \sin k\theta$ may be suitable when symmetric boundary conditions at $\theta = \pi/2k$ are desired.

If the singularity ray is located at (θ_1, ϕ_1), it is possible to choose, e.g.

$$\rho = \{(\theta - \theta_1)^2 + [(\phi - \phi_1) \sin \theta_1]^2\}^{1/2}. \tag{9}$$

Generalization to the case of several singularity rays contained within the domain on the unit sphere is obvious. For three rays, e.g.

$$u(\theta, \phi, r) = r^\lambda F(\theta, \phi) = r^\lambda \rho_1^{p_1} \rho_2^{p_2} \rho_3^{p_3} U(\theta, \phi) \tag{10}$$

where

$$\lambda = n + p_1 + p_2 + p_3 \tag{11}$$

p_1, p_2, p_3 being known exponents for the three rays and ρ_1, ρ_2, ρ_3 functions of the same type as $\rho(\theta, \phi)$ was before.

Now consider a singularity ray which is placed into the pole of a spherical coordinate system (e.g. ray 00′ in Fig. 2). In the plane (θ, ϕ) the pole appears as a straight line segment $\theta = 0$ with end points given by the angles ϕ_1, ϕ_2 forming the crack or notch that creates the singularity (Fig. 3). This line segment is a part of the boundary of domain Ω in the plane (θ, ϕ) on which function $U(\theta, \phi)$ has to be solved. It is obvious that a certain boundary condition must be imposed at this line segment (0′0̄′ in Fig. 3). The boundary condition may be deduced from the fact that U must be proportional to the function f_1 from equation (2) in the vicinity of $\vartheta = 0$. In equation (2) f_1 depends only on ϕ, i.e. is independent of θ. Hence, the condition

$$\partial U / \partial \theta = 0 \quad \text{at } \theta = 0 \tag{12}$$

must be satisfied.

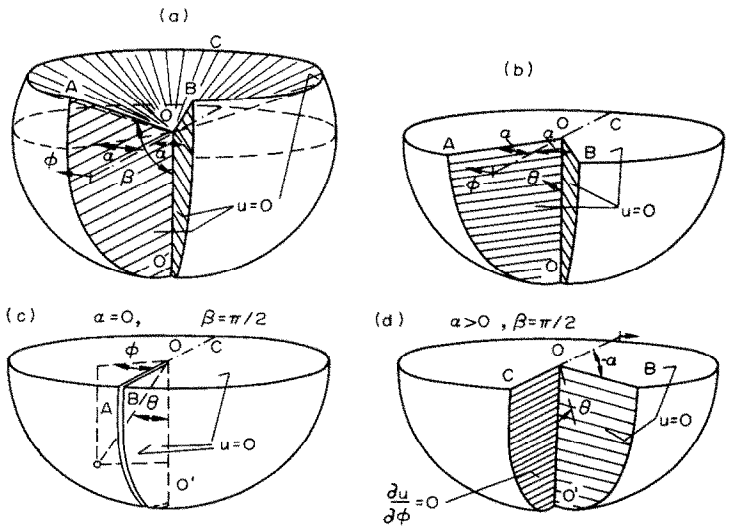

Fig. 2. Various cases of a notch or crack ending into a conical or planar surface. (The sphere is not the body surface and serves only for visualizing the situation in spherical coordinates.)

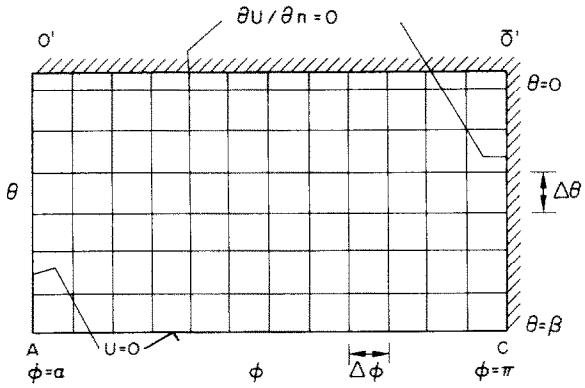

Fig. 3. Domain $0'AC0'$ from Fig. 2 visualized in (θ, φ) plane, with a nodal net used for numerical solution.

DIFFERENTIAL EQUATION OF THE PROBLEM AND VARIATIONAL FORMULATION

Substitution of equation (6) into equation (1) yields, after rearrangement and simplification, the partial differential equation:

$$\rho^2 \frac{\partial^2 U}{\partial \theta^2} + \frac{\rho^2}{\sin^2 \theta} \frac{\partial^2 U}{\partial \phi^2} + \left(2p\rho \frac{\partial \rho}{\partial \theta} + \rho^2 \cot \theta\right) \frac{\partial U}{\partial \theta} + \left\{\lambda(\lambda+1)\rho^2 + p\left[\rho \frac{\partial \rho}{\partial \theta} \cot \theta + (p-1)\left(\frac{\partial \rho}{\partial \theta}\right)^2 + \rho \frac{\partial^2 \rho}{\partial \theta^2}\right]\right\} U = 0. \tag{13}$$

In the special case where $\rho = \sin \theta$, equation (13) becomes

$$\sin^2 \theta \frac{\partial^2 U}{\partial \theta^2} + \frac{\partial^2 U}{\partial \phi^2} + \left(p + \frac{1}{2}\right) \sin 2\theta \frac{\partial U}{\partial \theta} + \{[\lambda(\lambda+1) - p(p+1)] \sin^2 \theta + p^2\} U = 0. \tag{14}$$

The problem consists in finding a nonzero solution of equation (13) or (14) which satisfies the boundary conditions at a surface formed by the radial rays and gives the smallest positive real part of λ.

It should be noted that for $\theta \to 0$, equation (14) becomes $\partial^2 U/\partial \phi^2 + p^2 U = 0$, which gives $U \sim \cos p\phi$, as is required by equation (2).

For numerical solution, the variational formulation is of particular interest. The functional associated with the Laplace equation is known to be

$$\mathcal{W} = \int_V \frac{1}{2} (\text{grad } u)^2 \, dV + \mathcal{W}_1 = \frac{1}{2} \int_V \left[\left(\frac{\partial u}{\partial r}\right)^2 + \left(\frac{1}{r} \frac{\partial u}{\partial \theta}\right)^2 + \left(\frac{1}{r \sin \theta} \frac{\partial u}{\partial \phi}\right)^2\right] dV + \mathcal{W}_1 \tag{15}$$

where V = volume, $\mathcal{W}_1$ = certain integral over the boundary surface. The functional which is associated with equation (13) or (14) may be obtained by reducing functional $\mathcal{W}$ to a two-dimensional one. In conformity with the separation of variables by substitution (6), the minimizing condition for $\mathcal{W}$ may be considered to be of the form $\delta(\delta_r \mathcal{W}) = 0$ where δ_r is the variation with regard to functions of r, and δ is the variation with regard to functions of θ and ϕ. Thus, according to (15) and (7),

$$\delta \int\int\int_V \left[R'F^2(\delta_r R)' + \frac{R}{r^2}\left(\frac{\partial F}{\partial \theta}\right)^2 \delta_r R + \frac{R}{r^2 \sin^2\theta}\left(\frac{\partial F}{\partial \phi}\right)^2 \delta_r R \right] r^2 \sin\theta \, d\theta \, d\phi \, dr + \delta(\delta_r \mathcal{W}_1) = 0 \quad (16)$$

where $R = r^\lambda$, $R' = dR/dr$. Integration by parts with respect to $(\delta_r R)'$ provides

$$\int_r r^\lambda \left\{ \delta \int\int_\Omega \left[-\lambda(\lambda+1)F^2 + \left(\frac{\partial F}{\partial \theta}\right)^2 + \frac{1}{\sin^2\theta}\left(\frac{\partial F}{\partial \phi}\right)^2 \right] \sin\theta \, d\theta \, d\phi \right\} \delta_r R \, dr + \delta(\delta_r \mathcal{W}_1) = 0 \quad (17)$$

where Ω is the given domain on the unit sphere. Since this equation must be satisfied for any variation $\delta_r R$ as a function of r, the minimizing condition reduces to $\delta W = 0$, where W is the following functional

$$W = \int\int_\Omega \frac{1}{2}\left[\left(\frac{\partial F}{\partial \theta}\right)^2 + \frac{1}{\sin^2\theta}\left(\frac{\partial F}{\partial \varphi}\right)^2 - \lambda(\lambda+1)F^2 \right] \sin\theta \, d\theta \, d\varphi + W_1 \quad (18)$$

in which $F = \rho^p U$; W_1 is a certain integral arising from $\mathcal{W}_1$. Because the surface of the body in three dimensions consists of radial rays, W_1 represents a certain contour integral along the boundary of the domain Ω. The foregoing simple derivation is, of course, not rigorous, but it is easy to verify using standard procedures that equation (13) is indeed associated with the variational principle $\delta W = 0$.

SOME CASES ADMITTING SIMPLE ANALYTICAL SOLUTIONS

Consider solutions of equation (14) which have the form

$$U(\theta, \phi) = Y(\theta) \sin p\phi. \quad (19)$$

This obviously satisfies the boundary conditions

$$U = 0 \text{ at } \phi = 0 \text{ and at } \phi = 2(\pi - \alpha) = \pi/p \quad (20a)$$

or

$$U = 0 \text{ at } \phi = 0 \text{ and } \partial U/\partial\phi = 0 \text{ at } \phi = \pi - \alpha = \pi/2p \quad (20b)$$

that is, $U = 0$ at the planes $00'A$ and $00'B$ in Fig. 2 where α and p are related as given by equation (2). Thus, if domain Ω on the unit sphere is rectangular in θ and ϕ (Fig. 3), i.e.

$$0 \leq \phi \leq \pi/p, \quad 0 \leq \theta \leq \beta \quad (21)$$

function $Y(\theta)$ in (19) needs to satisfy only the boundary conditions on $\theta = 0$ and $\theta = \beta$. Considering that there is a free surface at $\theta = \beta$ (a cone, and for $\beta = \pi/2$ a plane; Fig. 2), and taking equation (12) into account, one may write

$$\partial U/\partial\theta = 0 \text{ at } \theta = 0, \quad U = 0 \text{ at } \theta = \beta. \quad (22)$$

Thus, it is necessary and sufficient that $Y(\theta)$ fulfill the boundary conditions:

$$\partial Y/\partial\theta = 0 \text{ at } \theta = 0, \quad Y = 0 \text{ at } \theta = \beta. \quad (23)$$

For $\alpha < \pi/2$ there is a single singularity ray in this problem, the ray 00′ in Fig. 2, and for $\alpha \geq \pi/2$ there is none. (On rays $0A$, $0B$ there is no singularity.) Substituting equation (19) into (14), equation (14) is found to be satisfied if

$$\frac{d^2Y}{d\theta^2} + (2p+1)\cot\theta\frac{dY}{d\theta} + [\lambda(\lambda+1) - p(p+1)]Y = 0. \tag{24}$$

Upon introduction of a new independent variable $x = \sin^2\theta$, equation (24) may be transformed to the form

$$x(1-x)\frac{d^2Y}{dx^2} + \left[p+1-\left(p+\frac{3}{2}\right)x\right]\frac{dY}{dx} + \frac{\lambda(\lambda+1)-p(p+1)}{4}Y = 0 \tag{25}$$

which is seen to be a special form of the hypergeometric (Gauss) differential equation. The solution of this equation [12] leads to hypergeometric functions and it can be shown that it may be expressed in terms of elementary functions only if $\beta = \pi/2$, that is if the conical surface degenerates into a plane (Fig. 2b). Then the root λ having the smallest real part is obtained as

$$\lambda = p+1 \tag{26}$$

and the corresponding solution is

$$u(\theta, \phi) = Cr^{p+1}(\sin\theta)^p \cos\theta \sin p\phi \tag{27}$$

where C=an arbitrary constant. Equation (27) can be proved by substitution into (14). Note that, for any angle α, λ is greater than 1.

An interesting result is thus obtained: the gradient singularity at the ray (edge of a crack or notch, e.g.) disappears at the surface of the body (cases in Fig. 2b, c, d).

One important case is the half-space $-\pi \leq \phi \leq 0$ whose boundary conditions at the surface $\phi = 0$ are $u = 0$ on the infinite wedge $0 \leq \theta \leq 2\beta$ and $\partial u/\partial n = \partial u/\partial\phi = 0$ on the rest of the surface (Fig. 11a). Simple analytical solutions exist [11] for two limiting cases:

$$u = C\ln\left(\tan\frac{\theta}{2}\right) \quad \text{for } \beta \to 0 \quad (\lambda = 0) \tag{28}$$

$$u = Cr\sin\theta\sin\phi \quad \text{for } \beta \to \pi \quad (\lambda = 1) \tag{29}$$

and, of course, for the case $\alpha = \pi/2$ in which the problem reduces to a plane one and has a well known solution yielding $\lambda = \frac{1}{2}$.

REDUCTION TO A NONLINEAR EIGENVALUE PROBLEM FOR A MATRIX

Because function $U(\theta, \phi)$ has no gradient singularities, standard numerical methods may be applied to its determination. For complicated geometries of the domain Ω on the unit sphere, the most versatile approach will certainly be the finite element method. However, development of finite elements on the basis of the functional (18) exceeds the scope of this paper and will be treated separately. For domains of simpler geometries,

the use of the finite difference method appears to be easier and has been adopted for all computer studies reported herein. The differential equation (14) or (13) is replaced by its finite difference approximation in terms of nodal values U_i ($i = 1,2,\ldots$) and is written for all nodes of the chosen network inside the domain Ω. Some of the equations involve nodal points outside the boundary for which further equations expressing the boundary conditions must be added.

Application of the finite difference method, as well as the finite element method, yields a large system of N homogeneous linear algebraic equations for values U_j of function U in the nodes $j = 1,2,\ldots, N$,

$$\sum_{j=1}^{N} A_{ij}(\lambda) U_j = 0 \quad (i = 1, 2, \ldots N). \tag{30}$$

The determinant of matrix A_{ij}, in general complex, must vanish for a non-zero solution to exist. The problem is thus reduced to finding a root λ having the smallest positive real part. The solution is complicated by the large size of matrix $[A_{ij}]$ needed for accurate results, and also by the fact that A_{ij} are nonlinear functions of λ (polynomials). Various methods of solution are possible.

Method A. Reduction to a matrix eigenvalue problem

Noticing that equation (13) or (14) involves λ solely through the term $\lambda(\lambda+1) = \mu$, matrix A_{ij} is a linear function of μ. Furthermore, if the finite difference method is used, μ appears only in the diagonal coefficients of A_{ij}, and if the equations expressing the boundary conditions are eliminated, μ appears in all diagonal coefficients. Mere division of each equation by the coefficient at μ reduces the matrix A_{ij} to the form:

$$A_{ij}(\lambda) = K_{ij} - \mu\delta_{ij} \tag{31}$$

where K_{ij} is a matrix which is independent of λ, and $\delta_{ij}=1$ for $i=j$, $\delta_{ij}=0$ for $i \neq j$. Thus, a standard eigenvalue problem in μ for a real, general (nonsymmetrical) matrix is obtained. There are two roots λ which correspond to each root μ,

$$\lambda = -\tfrac{1}{2} \pm \sqrt{\tfrac{1}{4} + \mu}. \tag{32}$$

If the roots λ are all real, the smallest positive λ evidently corresponds to the smallest μ ($\pm$ being replaced by $+$). But this is not true in the case of complex roots and all roots μ must be checked to determine the smallest $Re(\lambda)$.

For the solution of the eigenvalue problem obtained, standard subroutines are available [3, 6, 10, 15]. Nevertheless, even with the contemporary electronic computers it is difficult and costly to exceed 150 equations, approximately, which usually suffices for accurate but not highly accurate results. The cost is also substantially increased by the fact that for the finite difference method, matrix A_{ij} is non-symmetric.

The finite element method, which may be based on minimizing the functional (18), yields symmetric matrices A_{ij} and K_{ij}. However, in contrast with the finite difference method, μ no longer appears exclusively in the diagonal terms of A_{ij} and inversion of a matrix of the size $N \times N$ is necessary to obtain a standard eigenvalue problem in μ.

Taking advantage of the sparsity of matrix A_{ij}, a much larger matrix can be stored in

rapid access memory and the eigenvalue could be obtained by iteration [3, 6, 10]. However, this would be economical only for the eigenvalue of largest absolute value. Attempts have been made to recast the problem in terms of the highest eigenvalue, e.g. replacing λ with $1/\gamma$ and linearizing with respect to γ. It appears, however, that this approach is impossible because there are always some spurious negative roots whose absolute value is larger than the largest positive γ.

Method B. Conversion to nonhomogeneous equation systems

(a) *The case of real root.* In this method, which has been used with success [2] to solve buckling problems for very large elastic structural systems leading to equations of type (30), a certain value λ_0 is first chosen and all coefficients $A_{ij}(\lambda_0)$ are evaluated. One equation, whose number will be referred to as k, is replaced by the equation $U_k = 1$, which makes the system nonhomogeneous. Normally the matrix of the new system is nonsingular and all U_i ($i = 1,2, \ldots, N$) may be solved using the standard subroutines for systems of linear equations. The obtained values of U_i are then substituted into the original k^{th} equation, previously replaced, and the corresponding right-hand side $\Sigma_j A_{kj} U_j = Q$ is computed. In general Q will be nonzero and the aim is to find the smallest value of λ for which $Q = 0$. This may be done by the regula falsi method. Several values of λ_0 are selected and the plot of Q versus λ_0 is imagined as shown in Fig. 6. Subsequent choices of λ_0 are made by linear interpolation. Good accuracy and convergence is achieved only when the k^{th} equation is chosen in such a manner that no $|U_i|$ is much larger than U_k.

From computer studies it has been found that the radius of convergence of this method is sometimes quite small. The interval of interest, such as $0 \leqslant \lambda \leqslant 2$, must be scanned in small steps of λ, about 0·05, to obtain a good initial guess of λ. Only then may the automatic improvements of λ by the regula falsi method be started. This is obvious from the sharply varying slope of the plot b in Fig. 6 (although there exists cases of slowly varying slope, as is shown by curve c in Fig. 6). Much care is needed to avoid missing the smallest root. Nevertheless, if a great number of problems with the given data varying in small steps are being solved, as in the studies reported herein, an approximate value of λ is usually known in advance and scanning of the large interval may be skipped. It is because of this fact that this method is usually much more economical than the general programs for eigenvalues. Moreover, in contrast with method A, this method allows handling up to one or two thousand equations without great difficulties (using either various elimination methods for banded matrices with tape storage or the sparse matrix storage in rapid access memory combined with an iterative solution).

If no estimate of λ is available, computationally the most efficient procedure is a combination of methods A and B. First, method A with a low number of nodes is used to obtain an approximate value of λ and the solution is then refined to a high accuracy using method B with a large number of nodes.

As an alternative to method B, it is also possible to apply the regula falsi method to the plot of the determinant of A_{ij} versus λ. But the slope of this plot usually varies even more rapidly and the convergence properties were found to be poorer than in method B.

(b) *The case of complex root.* When root λ of the smallest real part happens to be complex, a similar method may be used. In this case U_i, as well as matrix A_{ij} depending on λ, must be considered as complex. The objective is to find complex λ_0 for which

$Q = 0$. First, an arbitrary value of $Im(\lambda_0) = X$ is chosen and, keeping it fixed, the plot of $Re(Q)$ versus $Re(\lambda_0)$ is examined, choosing various values of $Re(\lambda_0)$. The point at which $Re(Q) = 0$ may be found by the regula falsi method and the corresponding $Im(Q)$ denoted as Y. The foregoing procedure is then repeated for various $Im(\lambda_0) = X$ and, considering the plot of Y versus X, the point at which $Y = 0$ (and $Q = 0$) is again found by the regula falsi method.

The fact that the regula falsi method must be applied in two dimensions makes the computations much more expensive than in the case of a real λ. Moreover, because the matrix is complex, the running time of each equation system is longer. Nevertheless, using tape storage or compact storage of the sparse matrix, much larger systems can be handled than with method *A*.

Method C. Successive linearizations with respect to λ

If the technique presented here is applied in elasticity, A_{ij} will usually consist of general polynomials in λ, complex or real. Method *B* will still be applicable, but instead of Method *A* successive solutions of eigenvalue problems will be required. Since A_{ij} are, in general, analytic functions of a complex variable λ, expansion in a Taylor series about a chosen complex λ_0 is possible. The series may be truncated after the second term to achieve linearization. Equations (30) are then reduced to the form

$$\sum_{j=1}^{N} (A^0_{ij} - \lambda' A'_{ij}) U_j = 0 \quad (i = 1,2,\ldots N) \tag{33}$$

where $\lambda' = \lambda_0 - \lambda$, $A^0_{ij} = A_{ij}(\lambda_0)$, $A'_{ij} = -\partial A_{ij}(\lambda_0)/\partial\lambda$. Multiplication of matrix equation (33) by the inverse of A'_{ij} then produces a standard eigenvalue problem, in general with a complex matrix. The objective is to find λ_0 for which $\lambda' = 0$. This can be achieved by application of the regula falsi method, in the same procedure as the condition $Q = 0$ is achieved in method *B*.

This method has so far been tested only in the problems with real λ as reported in the sequel. The convergence was rapid and the radius of convergence appeared to be quite large, that is the method automatically converged even if the initial guess of λ_0 was very poor (e.g. 0·2 in the case of plot (a) in Fig. 6). This is due to the slow change of the slope in this plot.

APPLICATION AND RESULTS OF NUMERICAL STUDIES

Cracks and notches ending at a plane or conical surface

To examine the numerical methods described above, the cases whose exact solution is known were solved first. These are the cases shown in Fig. 2 and characterized by boundary conditions (20a) and (22). There is only one singularity ray 00′ in these problems. The domain Ω is given by equation (21) and is rectangular in terms of θ and ϕ, as shown in Fig. 3. The domain was subdivided by a rectangular network with steps $\Delta\phi = (2\pi - \alpha)/2n$, $\Delta\theta = \frac{1}{2}\pi/(n + \frac{1}{2})$. It is noteworthy that no interior nodes of the network may be placed on the boundary line $\theta = 0$ because the finite difference equations for the nodes on this line do not involve any node with $\theta \neq 0$. However, these nodes may be considered as exterior nodes of the network used in formulating the boundary condition (as has been done in computing Table 2).

The solutions were carried out for various sizes of the step. The results for $\alpha = 0$, given in Fig. 7, indicate an excellent convergence of λ to the exact value 1·5 resulting

from equations (26) and (2). For 72 equations the error is 0·4 per cent and for 1152 equations it is 0·04 per cent. The convergence is monotonous and from the slope of the line in Fig. 7 it may be inferred that the error $\approx$ (step size)$^{1.9}$, that is, the convergence is almost quadratic. A similar picture is obtained for other values of α.

The solutions were also computed for non-zero values of β, that is, the cases of cracks or notches ending at the apex of a conical surface, which do not admit simple analytical solutions. The results are plotted in Fig. 4 and some of the results are tabulated in Table 1 (where three decimals are believed to be correct).

The results for $\beta \neq 0$ were compared and agreed with one-dimensional finite difference solutions of the ordinary differential equation (24). (For $\alpha = 0$, $\beta = \pi/2$, step $\Delta\theta = \beta/50$ gave $\lambda = 1{\cdot}4998$, which is only 0·013 per cent in error.) For several cases, the eigenstates, as characterized by function $Y(\theta)$ in equation (19), are plotted in Fig. 5. As a check, some solutions have also been run with $\rho^p = \sqrt{\vartheta}$ and the results were identical.

It is interesting to note that at a certain value $\beta > \pi/2$, depending on α, λ becomes less than 1·0 so that grad u is singular at point 0. But the singularity is always weaker than at the edge 00′ (see Fig. 4).

Cracks ending obliquely at a halfspace surface

The general method presented herein was further applied to the case shown in Fig. 8b, which is equivalent to the case in Fig. 8a where the boundary conditions are also given. There is only one singularity ray 00′ in this problem, with $p = \frac{1}{2}$ from equation

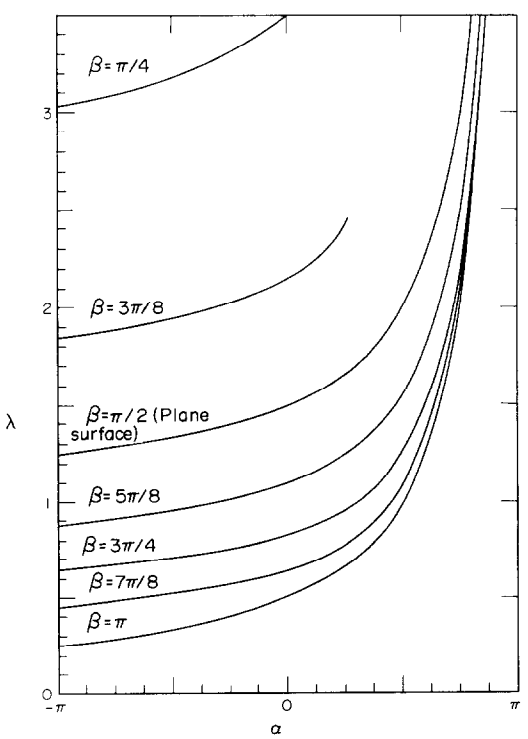

Fig. 4. Singularity strength for cases shown in Fig. 2.

Table 1. Values of λ for various α and β in the problem shown in Fig. 2

α \ β	$\pi/4$	$3\pi/8$	$\pi/2$	$5\pi/8$	$3\pi/4$	$7\pi/8$	π
$-\pi$	3·031	1·846	1·250	0·888	0·641	0·455	0·250
$-\pi/2$	3·189	1·953	1·333	0·958	0·704	0·515	0·333
$-\pi/4$	3·314	2·039	1·400	1·015	0·755	0·565	0·400
0	3·500	2·167	1·500	1·100	0·833	0·642	0·500
$\pi/8$	3·631	2·257	1·571	1·162	0·890	0·699	0·571
$\pi/4$	3·806	2·449	1·667	1·244	0·967	0·778	0·667

(2). The pole of the spherical coordinates is conveniently placed into this ray. Then, using $\rho = \sin\vartheta$, the problem is again governed by the differential equation (14). Ω is the domain $0'ABCD0'$ (or $0'AECD0'$) in Fig. 8 as is shown in plane (θ, φ) in Fig. 10. The boundary conditions are $\partial u/\partial\varphi = 0$ on side $DC0'$ (plane of symmetry), $\partial u/\partial\vartheta = 0$ at the pole $0'$ (side $0'\bar{0}'$ in Fig. 10), $u = 0$ on side $0'A$ (crack surface) and $u = 0$ on side ABC (or AEC). The latter side appears in the plane (θ, φ) as the curve defined as follows:

$$\theta = \arctan(\tan\beta/\cos\varphi); \quad \text{if } \theta < 0 \text{ then } \theta \leftarrow \theta + \pi. \tag{34}$$

Formulation of the finite difference equivalents of the boundary condition $u = 0$ in terms of the nodal values near boundary ABC requires locating point (θ_c, φ_c) which is symmetrical with respect to plane ABC to a given outside node (θ_a, φ_a). To this end, the value of θ which corresponds to $\varphi = \varphi_a$ according to (34) is first calculated and, using spherical trigonometry, the following expressions are successively evaluated

$$\left.\begin{aligned} \cos\psi &= 1 - 2(\cos\beta\sin\varphi_a)^2 \\ \theta_c &= \arccos[\cos\theta_a\cos(\theta_a - \theta) + \sin\theta_a\sin(\theta_a - \theta)\cos\psi] \\ \varphi_c &= \varphi_a + \arcsin[\sin(\theta_a - \theta)\sin\psi/\sin\theta_c]. \end{aligned}\right\} \tag{35}$$

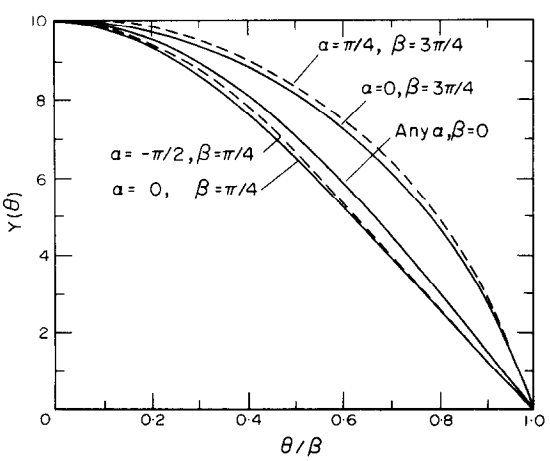

Fig. 5. Plot of function $Y(\theta)$ from equation (19) for some cases shown in Fig. 2.

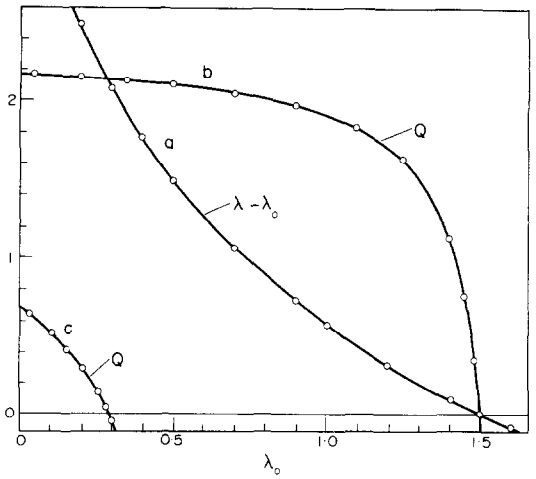

Fig. 6. Examples of dependence of λ and parameter Q upon λ_0 in methods A and B for solving equations (30). (Curves a, b correspond to Fig. 2c, curve c to Fig. 12a.)

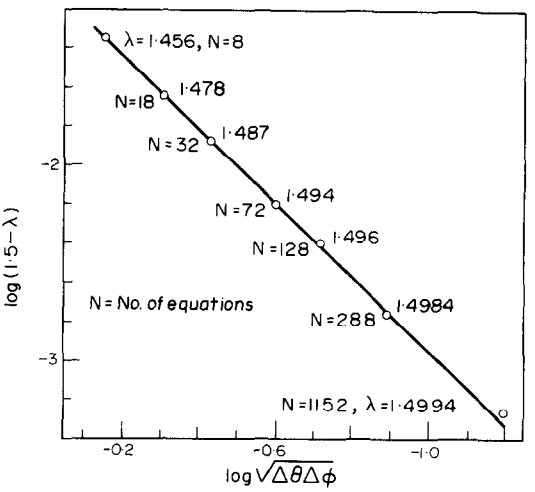

Fig. 7. Convergence of λ to the exact value 1·5 with diminishing step size of the net, for the case in Fig. 2c.

The U-value at point (θ_c, φ_c) is then related by linear interpolation to the U-values at the nearest three interior nodes p, q, r using area coordinates in the triangle pqr, i.e. $U_c = (a_{cqr}U_p + a_{crp}U_q + a_{cpr}U_r)/a_{pqr}$ where a_{cqr} etc. are the areas of the triangles indicated by subscripts. The boundary condition $U = 0$ is expressed in the form $U_a = -U_c(\sin\theta_c/\sin\theta_a)^p$.

Introducing finite difference grids with 80–100 nodes, the problem has been solved for various values of β. The values of λ of the smallest real part are all real and the computer results are shown as points on curve a in Fig. 9. The limiting values $\lambda = 1$ and 2 for $\beta \to 0$ and $\beta \to \pi$ result from equation (2) for the plane problem. The value $\lambda = 1{\cdot}5$

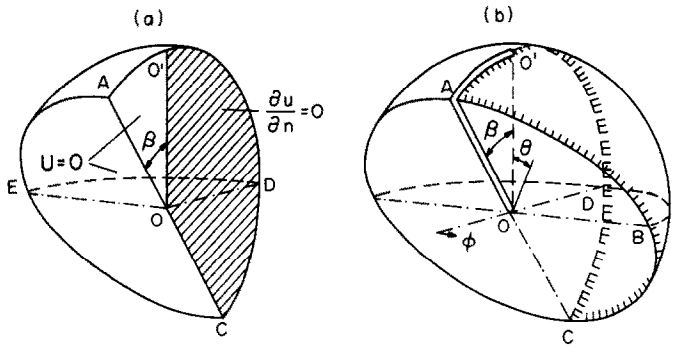

Fig. 8. (a) A quarterspace with boundary conditions giving rise to singularity on line 00'. (b) A halfspace with a crack whose edge is not perpendicular to the surface.

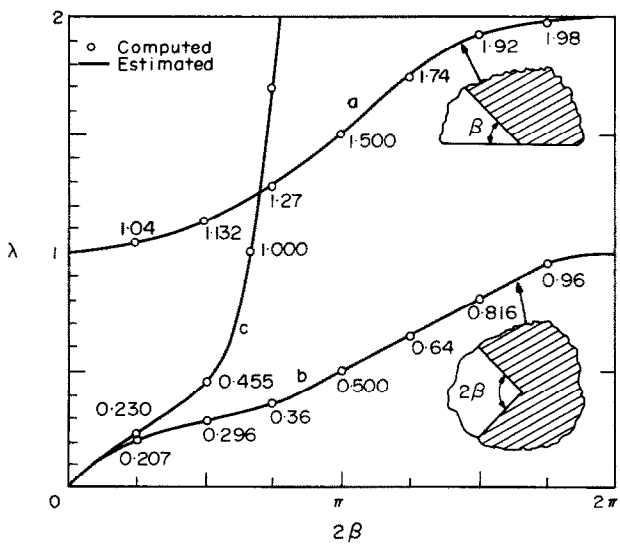

Fig. 9. Smallest real root λ for cases shown in Fig. 11 (curve b), Fig. 8 (curve a) and Fig. 13 (curve c).

for $2\beta = \pi$ agrees with the result from Fig. 4. It is noteworthy that the singularity on the ray 00' disappears at the surface of the halfspace (Fig. 8b) for any angle β. The eigenstates $U(\theta, \varphi)$ for two special cases are drawn in Fig. 10. For the case $\beta = \pi/4$ (Fig. 12a) it has been verified by method A that no complex roots exist. This case has also been analyzed by method B with grid $\Delta\varphi = \pi/24$, $\Delta\theta = \pi/26$ (359 nodes), which yielded $\lambda = 1{\cdot}131$, while the coarser grid ($\Delta\varphi = \pi/12$, $\Delta\theta = \pi/13$) resulted in $\lambda = 1{\cdot}128$ (the second and third smallest λ was 2·25 and 2·95). Assuming a similar convergence pattern as in Fig. 7, the correct value can be estimated as $\lambda = 1{\cdot}131 + 0{\cdot}001$, or $\lambda = 1{\cdot}132$.

Elastic stresses under wedge-shaped stamps or at crack edge corners. Wave scattering by corners.

Furthermore, the case of a rigid sliding stamp with wedge-shaped contact of an

Table 2. Nodal values of function U; (A)—Case in Fig. 10a ($p = 0{\cdot}5$); (B)—Fig. 12a ($p = 0{\cdot}5$); (C)—Fig. 12b ($p = 0{\cdot}5$); (D)—Fig. 14 ($p = 0{\cdot}5$); (E)—Fig. 11 for $\beta = \pi/8 (p = 2/3)$. Nodal coordinates are $\theta_k = K\Delta\theta$; $\varphi_i = J\Delta\varphi$ in cases (A), (B), (D) and (E); $\varphi_i = (J-1)\Delta\varphi$ in case (C); grid $\Delta\varphi = \pi/24$, $\Delta\theta = \pi/26$. In Table (C) the left and right of Fig. 14 are interchanged. The top row of each case was obtained by extrapolation.

K \ J	1	2	3	4	5	6	7	8	9	10	11	12	13	14	15	16	17	18	19	20	21	22	23	24
0	501	1001	1499	1995	2487	2974	3455	3927	4390	4841	5278	5697	6098	6476	6828	7151	7447	7708	7933	8120	8267	8373	8436	8458
1	478	956	1434	1912	2389	2865	3339	3809	4273	4729	5174	5604	6020	6414	6785	7128	7440	7717	7958	8159	8317	8431	8500	8523
2	409	821	1238	1663	2096	2540	2993	3454	3922	4397	4864	5331	5788	6231	6654	7051	7416	7745	8033	8275	8467	8606	8691	8719
3	333	672	1023	1390	1776	2183	2613	3064	3535	4020	4516	5016	5514	6002	6474	6921	7336	7712	8043	8322	8544	8706	8805	8838
4	258	510	789	1092	1427	1797	2202	2642	3114	3612	4130	4662	5197	5728	6245	6738	7199	7618	7988	8300	8551	8733	8844	8881
5	160	334	533	770	1051	1380	1760	2189	2661	3171	3710	4271	4841	5411	5969	6504	7005	7463	7868	8211	8486	8687	8809	8850
6	59	141	256	420	644	934	1288	1705	2178	2699	3258	3844	4446	5050	5645	6218	6756	7249	7685	8055	8351	8568	8700	8744
7			-47	40	206	457	787	1193	1667	2197	2774	3384	4013	4649	5276	5882	6452	6974	7437	7831	8146	8377	8517	8565
8						-50	258	655	1129	1669	2261	2891	3545	4207	4862	5495	6093	6641	7127	7540	7872	8114	8262	8311
9								91	568	1115	1721	2368	3042	3726	4404	5060	5680	6249	6754	7184	7528	7780	7934	7985
10									-15	539	1155	1816	2506	3207	3903	4577	5214	5799	6319	6761	7116	7375	7533	7586
11										-57	566	1237	1938	2652	3360	4047	4697	5293	5823	6274	6635	6900	7061	7115
12											-45	632	1339	2060	2776	3471	4127	4730	5265	5721	6087	6355	6518	6573
13												0	710	1433	2151	2847	3506	4110	4647	5104	5471	5740	5903	5958
14			(A) LAMBDA = 1.131										50	770	1485	2178	2832	3434	3968	4422	4787	5056	5216	5271
15														70	776	1460	2105	2698	3225	3673	4033	4295	4455	4509
16															21	691	1322	1902	2417	2854	3205	3462	3618	3671
17																-133	478	1039	1537	1961	2300	2548	2699	2749
18																	-436	100	578	981	1307	1544	1686	1736
19																				-95	213	435	569	613
0	461	925	1379	1832	2271	2704	3121	3524	3912	4283	4632	4962	5269	5551	5813	6048	6257	6439	6594	6722	6822	6892	6936	6950
1	448	933	1393	1844	2291	2723	3142	3546	3933	4302	4650	4977	5282	5563	5820	6052	6258	6438	6591	6716	6814	6884	6926	6940
2	480	959	1429	1892	2344	2782	3204	3609	3994	4359	4703	5023	5321	5594	5842	6065	6262	6434	6580	6699	6792	6859	6898	6912
3	494	987	1472	1945	2406	2849	3275	3680	4064	4425	4763	5077	5367	5632	5872	6087	6277	6441	6580	6694	6783	6846	6884	6897
4	514	1023	1523	2009	2478	2927	3356	3761	4143	4500	4832	5139	5421	5679	5911	6118	6301	6459	6593	6702	6787	6847	6884	6896
5	537	1067	1584	2084	2563	3018	3448	3853	4231	4584	4910	5210	5485	5735	5960	6160	6336	6489	6617	6722	6804	6862	6897	6908
6	565	1122	1659	2173	2661	3122	3554	3957	4331	4678	4998	5291	5559	5801	6019	6213	6383	6530	6654	6755	6833	6889	6923	6934
7			1759	2280	2777	3242	3674	4074	4444	4784	5097	5383	5643	5878	6089	6277	6442	6584	6704	6801	6877	6931	6963	6974
8						3381	3810	4204	4570	4907	5208	5486	5739	5968	6172	6354	6514	6651	6767	6862	6935	6987	7018	7029
9								4355	4711	5037	5333	5604	5849	6071	6269	6445	6600	6733	6846	6937	7008	7059	7089	7099
10									4871	5187	5474	5736	5974	6189	6381	6552	6702	6832	6941	7029	7098	7148	7177	7187
11										5356	5633	5887	6116	6324	6511	6677	6823	6948	7054	7140	7207	7255	7284	7293
12											5813	6057	6279	6480	6661	6822	6963	7085	7188	7272	7337	7384	7412	7421
13												6251	6465	6659	6835	6991	7128	7247	7347	7428	7492	7537	7564	7573
14			(B) LAMBDA = 0.2947										6679	6867	7036	7188	7321	7436	7534	7613	7675	7719	7745	7754
15														7108	7272	7419	7548	7660	7754	7832	7891	7934	7960	7968
16															7650	7792	7817	7925	8017	8092	8150	8191	8216	8224
17																8018	8138	8243	8332	8404	8460	8500	8524	8532
18																	8527	8630	8716	8785	8839	8877	8899	8907
19																				9255	9307	9343	9363	9370
0	8802	8784	8731	8645	8524	8369	8179	7956	7699	7409	7087	6733	6349	5935	5494	5026	4534	4019	3484	2931	2364	1784	1194	599
1	8739	8722	8671	8585	8467	8317	8134	7918	7670	7390	7078	6735	6362	5959	5525	5060	4569	4054	3517	2961	2389	1803	1208	606
2	8558	8538	8485	8400	8284	8138	7960	7750	7509	7237	6934	6601	6238	5845	5423	4973	4496	3991	3461	2905	2325	1724	1103	465
3	8310	8301	8272	8223	8151	8056	7931	7777	7591	7370	7112	6818	6482	6109	5697	5248	4764	4247	3700	3126	2529	1914	1284	644
4	8033	8028	8012	7983	7934	7863	7773	7663	7511	7322	7094	6827	6511	6155	5756	5316	4836	4319	3769	3189	2583	1956	1313	659
5	7711	7711	7711	7704	7692	7663	7609	7527	7410	7255	7056	6812	6521	6183	5797	5366	4891	4376	3824	3239	2626	1990	1337	671
6	7339	7344	7366	7394	7411	7401	7364	7298	7199	7068	6900	6693	6443	6152	5820	5398	4930	4417	3865	3277	2659	2016	1355	681
7				7039	7045	7150	7145	7107	7063	6986	6875	6735	6567	6367	6134	5825	5413	4951	4442	3891	3303	2682	2035	1364	687
8							6937	6984	6989	6940	6834	6668	6442	6156	5812	5411	4956	4452	3904	3316	2695	2045	1375	691
9									6811	6799	6723	6583	6379	6110	5780	5390	4944	4447	3903	3318	2697	2049	1378	693
10										6641	6595	6480	6296	6045	5729	5351	4915	4426	3888	3307	2690	2044	1375	691
11											6449	6358	6195	5961	5660	5295	4869	4389	3859	3285	2673	2032	1368	688
12												6217	6074	5857	5571	5219	4806	4336	3815	3250	2646	2012	1355	681
13													5932	5732	5462	5124	4724	4266	3757	3202	2609	1984	1336	672
14			(C) LAMBDA = 0.8150											5586	5332	5009	4624	4179	3683	3141	2561	1949	1312	660
15															5180	4874	4504	4075	3594	3067	2502	1904	1283	646
16																4717	4364	3952	3489	2979	2431	1851	1247	628
17																	4203	3810	3365	2875	2348	1788	1206	607
18																		3645	3223	2755	2251	1716	1157	582
19																					2139	1632	1101	554
0	613	1223	1822	2409	2975	3520	4036	4523	4973	5387	5758	6087	6368	6602	6784	6916	6995	7022						
1	617	1228	1830	2417	2986	3530	4047	4533	4983	5395	5766	6092	6372	6604	6786	6917	6996	7022						
2	624	1243	1850	2443	3015	3561	4079	4563	5011	5420	5787	6109	6385	6612	6791	6919	6996	7022						
3	634	1263	1879	2478	3055	3604	4123	4606	5052	5458	5820	6138	6409	6632	6807	6933	7008	7034						
4	648	1289	1916	2524	3107	3660	4179	4662	5106	5507	5865	6178	6445	6664	6836	6959	7032	7057						
5	665	1322	1963	2581	3171	3728	4249	4731	5172	5570	5924	6232	6494	6709	6877	6997	7069	7093						
6	688	1366	2022	2652	3249	3811	4333	4814	5252	5646	5995	6299	6556	6767	6932	7049	7120	7144						
7			2096	2739	3344	3909	4432	4912	5347	5736	6081	6380	6633	6840	7001	7116	7185	7208						
8						4027	4549	5026	5458	5843	6182	6476	6725	6928	7086	7199	7267	7289						
9								5160	5587	5967	6301	6590	6834	7034	7189	7299	7366	7388						
10									5738	6112	6440	6723	6963	7158	7311	7419	7485	7506						
11										6279	6601	6879	7113	7305	7455	7562	7626	7647						
12											6787	7059	7289	7478	7625	7730	7793	7814						
13												7269	7495	7680	7825	7928	7990	8010						
14			(D) LAMBDA = 0.4533										7736	7918	8060	8162	8223	8243						
15														8200	8340	8440	8500	8520						
16															8675	8773	8832	8852						
17																9178	9234	9253						
18																	9728	9748						
0	352	699	1045	1384	1717	2039	2351	2648	2933	3202	3455	3690	3909	4108	4290	4452	4596	4721	4826	4912	4979	5027	5056	5066
1	362	722	1075	1423	1764	2094	2396	2693	2974	3238	3486	3716	3927	4121	4296	4452	4590	4709	4810	4893	4957	5003	5030	5039
2	397	789	1171	1552	1929	2292	2534	2826	3094	3349	3589	3792	3984	4158	4314	4452	4573	4677	4764	4835	4890	4930	4953	4961
3	448	883	1297	1697	2049	2383	2686	2970	3227	3461	3673	3865	4039	4195	4333	4455	4562	4654	4730	4791	4841	4875	4896	4902
4			1472	1877	2244	2566	2854	3121	3357	3571	3763	3937	4092	4232	4356	4465	4560	4641	4709	4764	4807	4838	4856	4862
5						2765	3035	3274	3487	3679	3852	4007	4147	4272	4383	4481	4566	4639	4700	4750	4788	4816	4832	4838
6								3426	3615	3785	3940	4079	4205	4317	4417	4505	4582	4649	4706	4749	4784	4809	4824	4829
7									3741	3891	4029	4156	4267	4369	4459	4540	4610	4670	4721	4762	4794	4816	4830	4834
8										3997	4120	4233	4336	4429	4511	4584	4649	4704	4750	4788	4817	4838	4851	4855
9											4217	4320	4414	4498	4574	4641	4700	4751	4794	4829	4856	4875	4887	4891
10											4325	4418	4503	4580	4649	4711	4766	4813	4853	4885	4910	4928	4939	4943
11											4444	4527	4605	4675	4739	4796	4847	4891	4928	4958	4981	4998	5008	5012
12												4651	4722	4786	4845	4899	4945	4986	5021	5049	5071	5087	5096	5099
13												4792	4857	4917	4971	5020	5064	5102	5136	5161	5181	5196	5205	5208
14			(E) LAMBDA = .2057									4954	5014	5069	5120	5166	5206	5242	5272	5297	5316	5330	5338	5341
15													5198	5249	5296	5339	5377	5410	5438	5461	5479	5492	5498	5502
16													5414	5462	5506	5544	5581	5612	5638	5659	5674	5688	5695	5697
17													5672	5717	5759	5796	5828	5856	5880	5900	5916	5927	5933	5936
18														6029	6067	6101	6130	6156	6178	6196	6210	6220	6226	6228
19															6452	6481	6506	6528	6547	6563	6576	6585	6590	6592
20																6963	6983	7001	7017	7031	7042	7050	7055	7056
21																7605	7618	7632	7644	7653	7661	7665	7666	
22																	8460	8477	8488	8496	8502	8506	8507	
23																				9749	9753	9757	9758	

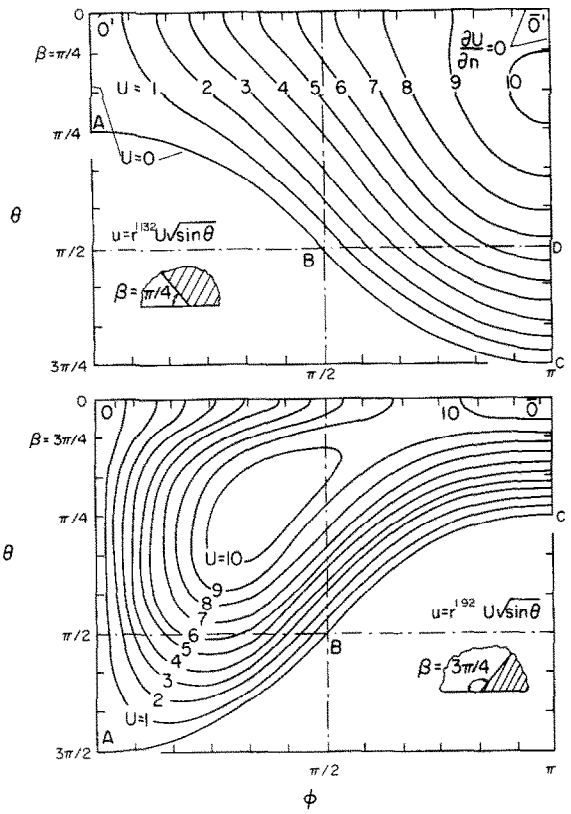

Fig. 10. Function U computed for the cases shown in Fig. 8 ($\rho^p = \sqrt{\sin\theta}$).

arbitrary angle, 2β, pressed upon the surface of an isotropic elastic half-space (Fig. 11a), has been studied. As is well known [4], this problem of elasticity may be reduced, with the help of Papkovich–Neuber potentials, to a potential theory problem, $\nabla^2 u = 0$. Introducing cartesian coordinates x, y, z and considering the half-space $z \geq 0$ or $0 \leq \varphi \leq \pi$, the boundary conditions at the halfspace surface are

$$u = 0 \text{ on } \mathcal{T} \quad \text{and} \quad \partial u/\partial z = 0 \text{ outside } \mathcal{T} \tag{36}$$

where $\mathcal{T}$ = the wedge-shaped domain below the stamp ($00'A0''$ in Fig. 11a). Also, at infinity, grad u is required to vanish. After solving for u, the displacements u_x, u_y, u_z in cartesian coordinates x, y, z at any point of the half-space $z \geq 0$ are given as [4]:

$$u_x = (1-2\nu)\int_z^\infty \frac{\partial u}{\partial x}\,dz - z\frac{\partial u}{\partial x}, \quad u_y = (1-2\nu)\int_z^\infty \frac{\partial u}{\partial y}\,dz - z\frac{\partial u}{\partial y}, \quad u_z = 2(1-\nu)u - z\frac{\partial u}{\partial z}, \tag{37}$$

where ν = Poisson's ratio of the material. The normal stress below the stamp is $\sigma_z = (\partial u/\partial z)E/(1+\nu)$ where E = Young's modulus.

This problem is equivalent to the case of an infinite elastic body containing a sharp crack whose edge forms a sharp corner of an arbitrary angle 2β (Fig. 11b). The body is subjected at infinity to uniformly distributed normal stresses perpendicular to the crack

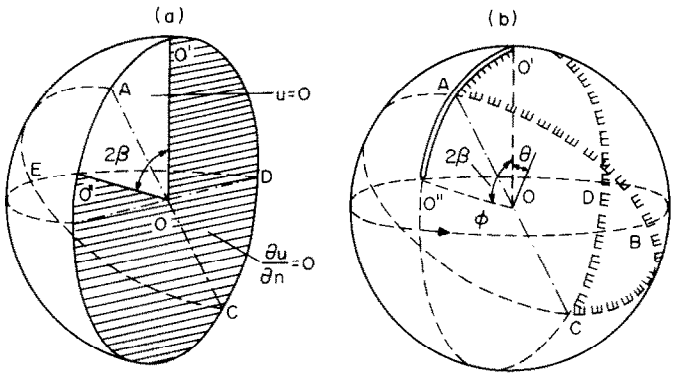

Fig. 11. (a) Wedge stamp contact (unshaded) upon elastic halfspace or, alternatively, a screen, scattering waves. (b) Crack corner in an infinite elastic space. (The sphere is not the body surface and serves only for visualizing the situation in spherical coordinates.)

plane. Furthermore, the near field in this problem happens to be the same as in the scattering of waves by a sharp corner of a screen [9].

Although in Fig. 11 there are two singularity rays, 00′ and 00″, each with $p = \frac{1}{2}$ from equation (2), the problem may be reduced to one with a single singularity ray, taking advantage of the fact that the solution u or F must be symmetrical with regard to plane $OABC$ in Fig. 11b. The formulation of the problem then differs from the previous case (Fig. 8) solely by the boundary condition on side ABC (or AEC) which reads:

$$\partial[(\sin\theta)^p U]/\partial n = 0 \tag{38}$$

where $p = \frac{1}{2}$ and n is the normal to the side AEC (normal on the sphere, not in the plane (θ, φ)). The finite difference formulation of the boundary condition is the same as in the previous case (Fig. 8, equations 34, 35), except that $U_a = U_c\ (\sin\theta_c/\sin\theta_a)^p$.

Computer results for grids with 80–100 nodes are shown by the points on curve b in Fig. 9. Note that the points adjacent to $\lambda = 0{\cdot}5$ fit a smooth curve passed through the well-known value of $\lambda = 0{\cdot}5$ for $2\beta = \pi$. The point $\lambda = 0$ for $\beta \to 0$ follows from equation (28), and $\lambda = 1$ for $\beta \to \pi$ results from equation (29). The eigenstates $U(\theta, \varphi)$ are shown for two special cases by lines of equal U-value in Fig. 12. It is worth noting that the computed variation of U along the top side $0'\bar{0}'$ of Fig. 12a or b is proportional to $\sin(\theta/2)$, as is required by equation (2).

The results prove that the singularity at the sharp concave ($2\beta < \pi$) corner 0 of a crack edge (Fig. 11b) in an elastic body is more severe ($\lambda < p$) than at a straight crack edge ($p = \frac{1}{2}$). This fact is of interest for fracture mechanics of brittle elastic materials. It shows that at a concave corner of the crack edge of a planar crack the crack will propagate faster or at a lower stress than at a straight edge. Obviously, this would tend to straighten the crack edge. A plane crack with a straight edge is thus more stable than a plane crack with zig-zag edge.

All roots have been computed by method B, restricting consideration to real λ. However, the case $2\beta = \pi/2$ has also been computed by method A; the result was identical and it was found that no complex roots λ exist in this case (similar to cases $2\beta = \pi$ and $\beta = \pi$).

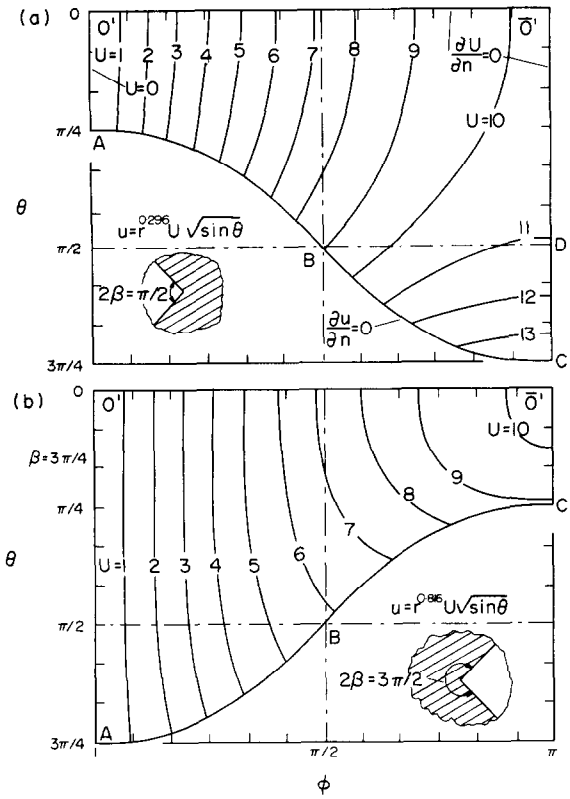

Fig. 12. Function U computed for the case shown in Fig. 11 ($\rho^p = \sqrt{\sin\vartheta}$).

All points on curve b in Fig. 9 have first been computed with grids $\Delta\varphi = \pi/12, \Delta\theta = \pi/13$ (80–100 nodes). For the case of a right-angled corner ($2\beta = \pi/2$; Fig. 12a) this grid (having 86 nodes, not counting those outside the domain) yielded $\lambda = 0{\cdot}2905$. This case has then also been computed with a grid $\Delta\varphi = \pi/24$, $\Delta\theta = \pi/26$ (having 359 nodes), which has resulted in $\lambda = 0{\cdot}2947$ (using method B). This differs by 0·0043 (i.e. 1·46 per cent) from the coarser grid. Nearly the same difference, namely 0·0044, is found between the grids with the same spacing in Fig. 7. Because the result for a grid with 359 nodes would be in Fig. 7 about 0·0015 below the exact value, it can be inferred that the correct value probably is $\lambda = 0{\cdot}2947 + 0{\cdot}0015$, i.e.

$$\lambda = 0{\cdot}296 \quad (\text{for } 2\beta = \pi/2). \tag{39}$$

(However, Radlow[9] deduced for this case analytically the value $Re(\lambda) = 0{\cdot}25$, whose difference from the present result is obviously much greater than the probable value of numerical error, and so reexamination of the analysis in[9] seems to be in order.) The second and third smallest λ, as found by method A with 86 nodes for $p = \frac{1}{2}$, are 1·43 and 2·03. It was also checked that higher p does not give smaller λ.

The case $2\beta = 3\pi/2$ (Fig. 12b) has also been computed with the finer grid, which has furnished $\lambda = 0{\cdot}8148$; assuming similar convergence behavior as before, the correct

value is $\lambda = 0{\cdot}815 + 0{\cdot}001 = 0{\cdot}816$. For $2\beta = \pi/4$, the finer grid yielded $\lambda = 0{\cdot}2057 + 0{\cdot}0015 = 0{\cdot}207$.

Rvachev's results for real roots[11], obtained by a mapping technique and the Galerkin method, differ considerably (by as much as 0·2) from curve b in Fig. 9. This is probably due to numerical error because Rvachev used only six unknown parameters.

For $\beta \to 0$, Aleksandrov and Babeshko[1] found λ to be complex, with $Re(\lambda) = -0{\cdot}5$, which overrides the value $\lambda = 0$ indicated by equation (28) and shown in Fig. 9. However, no cases with very small β have yet been run to verify this result. This will be postponed until the finite element formulation is completed (because refinement of the nodal network near side $0A$ in Fig. 10 will probably be desirable for high accuracy).

Singularity at the apex of pyramidal notches with three equal sides

The cases of pyramidal notches shown in Fig. 13 have 3 singularity rays and possess one plane of symmetry through each of the three edges, so that only the domain $0'ABCD0'$ needs to be considered. This domain includes only one singularity ray and the formulation of the problem is the same as for the cases shown in Fig. 11, discussed previously, except for two differences. First, angle 2α of the planes forming each radial edge depends on the apex angle 2β of each side, namely $\sin \alpha = 1/(2 \cos \beta)$, and the value of p is then given by equation (2). Second, the location of the right boundary in the (θ,φ) plane is different, as is shown in Fig. 14 for the case of the right-angled pyramidal notch ($2\beta = \pi/2$).

This case was analyzed only by method B, assuming λ to be real. The smallest roots computed with networks of about 80 nodes are given by the points on curve c in Fig. 9 and the eigenstate U for one case is shown in Fig. 14. Note that the cases $2\beta > 2\pi/3$ represent a convex solid pyramid rather than a concave notch. For $2\beta = 2\pi/3$ the pyramid degenerates into a planar surface ($\alpha = 0$), for which $\lambda = 1$. The case $\beta \to 0$ should give the same value as for curve b. (According to the result in[1], the values in Fig. 9 will possibly be overriden by some complex λ at $\beta \to 0$.) The right-angled pyramidal notch (Figs. 14 and 13a) has also been computed with a finer grid $\Delta\varphi = \pi/24$, $\Delta\theta = \pi/26$, which has yielded $\lambda = 0{\cdot}4533$. Assuming similar convergence behavior as before, the correct value is $\lambda = 0{\cdot}4533 + 0{\cdot}0015 = 0{\cdot}455$. For $2\beta = \pi/4$, the finer grid yielded $\lambda = 0{\cdot}2288 + 0{\cdot}0015 = 0{\cdot}230$ ($\alpha = 32{\cdot}765°$, $p = 0{\cdot}61127$).

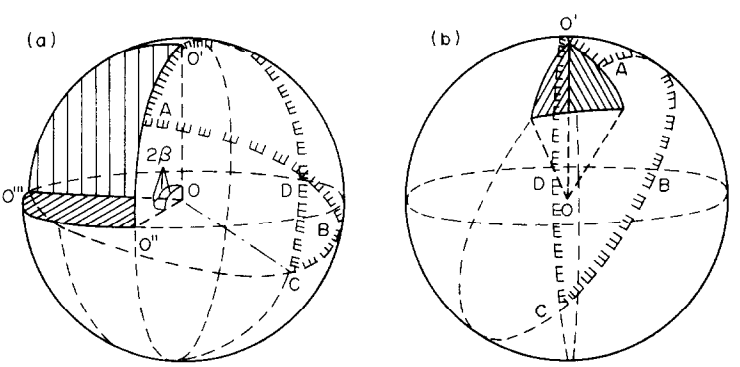

Fig. 13. Pyramidal notches with three sides of equal apex angle. (The sphere is not the body surface and serves only for visualizing the situation in spherical coordinates.)

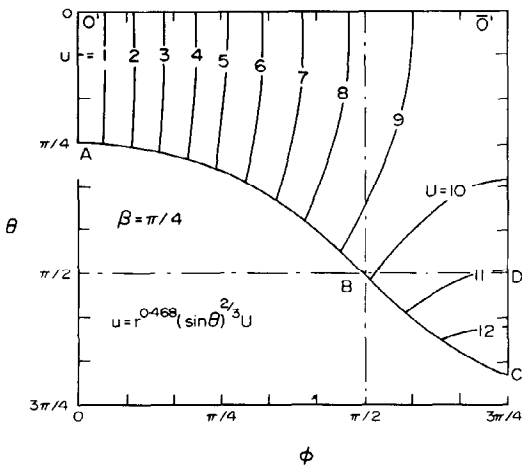

Fig. 14. Function U computed for the case shown in Fig. 13a ($\rho^{\pi} = (\sin\theta)^{2/3}$).

Development of singular finite elements and extensions to elasticity

It should be noted that knowledge of the dominant near-singularity field is all that is needed for the development of finite elements comprising the singularity, following the path shown, e.g. by Walsh[13]. Table 2 gives sufficient information for formulation of such elements for the most important cases. This brings within reach the numerical solutions by the finite element method for three-dimensional domains with arbitrary boundaries.

The general method presented can also be applied to problems of three-dimensional elasticity which are not reducible to potential theory problems. Here expressions of the form (6) or (10) augmented by rigid-body displacement terms for the neighborhood of the ray must be introduced for each of the three displacement components. The analysis may be based either on Navier's differential equations of equilibrium in spherical coordinates or the Papkovich–Neuber potentials. In either case the problem is reduced to three simultaneous second order partial differential equations in θ, φ for three functions with nonsingular gradients. Applying a numerical method, the problem is again reduced to the system of algebraic equations (30). But its matrix is about three times larger than for the same nodal network in a potential theory problem, has a wider band, and is less sparse. This will make computations more costly.

Application of the numerical method to singularities in plane elasticity

There is a number of unanalyzed singular problems in plane elasticity, especially in combinations of cracks, notches and bonded dissimilar materials. Analytical solutions are complicated and a great effort is being made to solve various cases one by one, as can be seen in the recent literature. The present method of numerical solution can be useful in all these problems, too. The technique of Knein[8] and Williams[13] reduces the plane problem to an ordinary rather than a partial differential equation. The system of equations (30) arising in numerical solution is therefore of a much smaller size, and usually also narrowly banded, which substantially simplifies computations according to methods *A*, *B* or *C* outlined previously.

CONCLUSION

Three-dimensional harmonic functions near termination or intersection of gradient singularity lines can be determined by the general numerical method presented herein. Knowledge of the near field will enable the development of finite elements comprising the singularity.

Acknowledgement—The author wishes to express his gratitude to his friend Dr. Leon M. Keer, Professor at Northwestern University, who called his attention to the present problem and helped by providing precious critical remarks in frequent discussions during the progress of the work. The computing funds were furnished by Northwestern University.

REFERENCES

[1] V. M. ALEKSANDROV and V. A. BABESHKO, *Prikl. Mat. Mekh.* **36**, 88 (1972). Translated in *J. appl. Math. Mech.*, 78 (1972).
[2] Z. P. BAŽANT and M. CHRISTENSEN, *Int. J. Solids Struc.* **8**, 327 (1972).
[3] L. COLLATZ, *Eigenwertaufgaben mit Technischen Anwendungen.* Akademische Verlagsgesellschaft Geest & Portig (1963).
[4] L. A. GALIN, *Contact Problems in the Theory of Elasticity* (in Russian). Gostechteorizdat (1953) Translated by H. MOSS, Dept. of Math., North Carolina State College, Raleigh (1961).
[5] L. A. GALIN, *Dokl. Akad. Nauk SSSR* **58**, (1947).
[6] V. N. FADDEEVA, *Computational Methods of Linear Algebra* (Translated from Russian) Dover (1959).
[7] S. N. KARP and F. C. KARAL, *Commun. pure Appl. Math.* **15**, 413 (1962).
[8] M. KNEIN, *Abhandlungen aus dem Aerodyn. Inst an der T. H. Aachen* **7**, 43 (1927).
[9] J. RADLOW, *Arch. ration. Mech. Analysis* **19**, 62 (1965).
[10] A. RALSTON, *A First Course in Numerical Analysis.* (Chapter 10). McGraw-Hill (1965).
[11] V. L. RVACHEV, *Prikl. Mat. Mekh.* **23**, 169 (1959).
[12] I. M. RYSHIK and I. S. GRADSTEIN, *Tables of Series, Products and Integrals*, VEB (1957).
[13] P. F. WALSCH, *Int. J. Solids Struct.* **7**, 1333 (1971).
[14] M. L. WILLIAMS, *J. appl. Mech.* **19**, 526 (1952).
[15] J. H. WILKINSON and C. REINSCH, *Handbook for Automatic Computation-Vol. II, Linear Algebra*, Springer (1971).
[16] E. A. KRAUT, *Bull. Seism. Soc. Am.* **58**, 1083, 1097 (1968).

(*Received* 18 *January* 1973)

Résumé—La fonction harmonique U au voisinage du point 0, à partir duquel part un rayon à singularité, est supposée être dominée par le terme $r^{\lambda}\rho^{p}U$ où r = distance du point 0, p = constante connue, et ρ une fonction choisie des coordonnées sphériques angulaires θ, φ telles que $u \sim (\rho r)^{p}$ au voisinage du rayon pour tout r fini. U est une fonction inconnue de θ, φ, pour laquelle une équation différentielle partielle avec les conditions aux limites, en particulier celles sur les rayons singuliers, et un principe variationnnel sont déduits. Parce que grad U est non singulier, une solution numérique est possible, utilisant, par exemple, les méthodes des différences finies ou des éléments finis. Ceci ramène le problème à celui de trouver un λ de partie réelle la plus petite et satisfaisant à l'équation Det $(A_{ij}) = 0$, où A_{ij} est une grande matrice dont les coefficients dépendent linéairement du $\mu = \lambda(\lambda + 1)$. En général λ et A_{ij} sont complexes. Des solutions peuvent être obtenues soit en se ramenant à un problème ordinaire de valeur propre de matrice pour μ, soit par des conversions successives à des systèmes d'équations linéaires non homogènes. Des études par ordinateur ont confirmees la faisabilité de cette méthode et ont montrées que des résultats de grande précision peuvent être obtenus. Des solutions pour des fissures et des entailles aboutissant à un plan, ou à une surface conique, et pour des fissures aboutissant obliquement à la surface d'un demi-espace, sont présentées. Dans ces cas, λ est réel et la singularité est toujours plus faible ($\lambda > p$) que sur la ligne singulière et peut même disparaître ($\lambda > 1$).

De plus, des contraintes élastiques sous l'effet d'un poinçon rigide, en forme de coin et glissant, ou à l'angle du bord d'une fissure ont été analysées, ainsi que des fonctions harmoniques pour des entailles pyramidales à trois côtés. Ici on avait $\lambda < p$.

Une solution analytique simple pour une classe de cas particuliers a également été trouvée. On l'a utilisé pour vérifier quelques uns des résultats numériques.

Zusammenfassung—Es wird angenommen, dass die harmonische Funktion u nahe dem Punkt 0, von dem ein einzelner Singularitätsstrahl ausgeht, durch den Ausdruck $r^{\lambda}\rho^{p}U$ beherrscht wird, wo r = Abstand vom Punkt 0, p = bekannte Konstante und ρ = gewählte Funktion von winkeligen Kugelkoordinaten θ, φ

so dass $u \sim (\rho r)^p$ nahe dem Strahl für jedes endliche r. U ist eine unbekannte Funktion von θ, φ, für die eine partielle Differentialgleichung mit Grenzbedingungen, besonders die an den Singularitätsstrahlen, und ein Variationsprinzip abgeleitet werden. Weil Gradient U nicht-singulär ist, ist eine numerische Lösung möglich, verwendend, zum Beispiel, die den Netzverfahren oder die Methode der endlichen Elementen. Dies reduziert das Problem auf das Finden von λ des kleinsten reellen Teiles, der die Gleichung Det $(A_{ij}) = 0$ befriedigt, wo A_{ij} *eine grosse Matrize ist, deren Koeffizienten linear von* $\mu = \lambda(\lambda + 1)$ abhängen. Im Allgemeinen sind λ und A_{ij} *komplex.*

Lösungen können entweder durch Reduktion auf ein gewöhnlicher Matrizeneigenwertproblem für μ erhalten werden, oder durch aufeinanderfolgende Umwandlungen auf nicht-homogene lineare Gleichungssysteme. Untersuchungen an Rechenanlagen bestätigten die Durchführbarkeit der Methode und zeigten, dass sehr genaue Resultate erhalten werden können. Es werden Lösungen für Risse und Kerben vorgelegt, die an einer Ebene oder Kegeloberfläche enden, und für Risse, die quer an einer Halbraumoberfläche enden. In diesen Fällen ist λ reell und die Singularität ist immer schwächer ($\lambda > p$) als an der die Singularitätslinie und kann sogar verschwinden ($\lambda > 1$). Weiter wurden elastische Spannungen unter einem keilförmigen starren gleitenden Stempel oder an der Ecke einer Risskante analysiert, wie auch harmonische Funktionen an dreiseitigen pyramidischen Kerben. Es wurde gefunden, dass $\lambda > p$ hier vorkommt. Es wurde auch eine einfache analytische Lösung für eine Klasse von Spezialfällen gefunden und wurde verwendet, um einige der numerischen Resultate zu prüfen.

Sommario—Si assume che la funzione armonica u, vicino al punto 0 da cui emana un raggio con singolarità singola, sia dominata dal termine $r^\lambda \rho^p U$ dove r è la distanza dal punto 0, p è una costante nota e ρ è una funzione scelta delle coordinate sferiche angolari θ e φ tale che $u \sim (\rho r)^p$ vicino al raggio per ogni valore finito di r. U è una funzione non nota di θ e φ per la quale vengono derivati un'equazione a differenziali parziali con condizioni allo strato limite, specialmente quelle sui raggi con singolarità, ed un principio variazionale. Poiché grad U non è singolare, una soluzione numerica è possibile, usando per esempio il metodo delle differenze finite o quello degli elementi finiti. Ciò riduce il problema a trovare il valore di λ della più piccola parte reale che soddisfa l'equazione Det $(A_{ij}) = 0$ dove A_{ij} è una grande matrice i cui coefficienti dipendono linearmente da $\mu = \lambda(\lambda + 1)$. In generale, λ et A_{ij} sono numeri complessi. Le soluzioni possono venir ottenute o per riduzione al problema del valore speciale di una matrice normale per μ, 0 per conversioni successive a sistemi di equazioni lineari non omogenee. Degli studi effettuati su calcolatori hanno confermato la praticabilità di questo metodo e hanno dimostrato che si possono ottenere risultati molto accurati. Vengono presentate soluzioni per fenditure e intagli terminanti su una superficie piana o conica, e per fenditure terminanti obliquamente sulla superficie di un semispazio. In questi casi λ è reale e la singolarità è sempre più debole ($\lambda > p$) che sulla linea di singolarità e può perfino scomparire ($\lambda > 1$). Sono state analizzate inoltre le sollecitazioni elastiche sotto uno stampo scorrevole rigido a forma di cuneo o su un angolo del bordo della fenditura, come pure le funzioni armoniche su intagli piramidali a tre facce. È stata inoltre trovata una semplice soluzione analitica per una classe di casi speciali, e la soluzione è stata usata per controllare alcuni dei risultati numerici.

Абстракт — Принято, что гармоническая функция u вблиз точки 0, от которого излучается один особенностный луч, подвержена к господству члена $r^\lambda \rho^p U$, где r = расстояние от точки 0, p = известное постоянное, ρ = выбор функции от угловых сферических координат θ, ϕ так, что $u \sim (\rho r)^p$ вблиз луча для любого конечного значения r. При этом U есть неизвестная функция от θ, ϕ, для которого дан вывод частного дифференциального уравнения с граничными условиями, в частности, для тех на особенностных лучах, а также выводится вариационный принцип. Так как *grad* U есть неособенная, возможно получить численное решение, применяя например методы конечных раздичий или конечных элементов. Поэтому проблема сводится к нахождниею λ для наименьшей реальной части, удовлетворающей уравнением Det $(A_{ij}) = 0$, где A_{ij} — большая матрица, коэффициенты которой зависят линейно от $\mu = \lambda(\lambda + 1)$. Вообще λ и A_{ij} — комплексными. Решения можно получить или приведением проблемы собственного значения стандартной матрицы относительно μ, или последовательными преобразованиями к системам неоднородных линейных уравнений. Из исследований компьютером подтверждена практическая осуществляемость метода, а также возможность получения высокоточных результатов. Представлены решения для трещин и надрезов, ограничивающихся у плоскости или конической поверхности, и для трещин, ограничивающихся косно у полупространственной поверхности. Во этих случаях λ есть реальное, а особенность всегда более слабое ($\lambda > p$), чем значение ее на особенностной линии, возможно и исчезание ее ($\lambda > 1$). Кроме того, проанализированы упругие напряжения под клин-образном, жестким, скользящим штампом, или во угле края трещины, и гармонические фунции трехгранных пирамидальных надрезов. Здесь установлено что $\lambda < p$. Получено и простое аналитическое решение для одного класса частных случаев, примененное для проверки некоторых численных результатов.